Quantum Electronics **45** (11) 1003–1009 (2015)

ACTIVE MEDIA

PACS numbers: 42.55.Ks; 42.60.Mi
DOI: 10.1070/QE2015v045n11ABEH015796

Gas-dynamic perturbations in an electric-discharge repetitively pulsed DF laser and the role of He in their suppression

P.A. Evdokimov, D.V. Sokolov

Abstract. **The gas-dynamic perturbations in a repetitively pulsed DF laser are studied using a Michelson interferometer. Based on the analysis of experimental data obtained in two experimental sets (working medium without buffer gas and with up to 90% of He), it is concluded that such phenomena as isentropic expansion of a thermal plug, gas heating by shock waves and resonance acoustic waves do not considerably decrease the upper limit of the pulse repetition rate below a value determined by the time of the thermal plug flush out of the discharge gap. It is suggested that this decrease for a DF laser with the SF_6–D_2 working mixture is caused by the development of overheat instability due to an increased energy deposition into the near-electrode regions and to the formation of electrode shock waves. Addition of He to the active media of the DF laser changes the discharge structure and improves its homogeneity over the discharge gape cross section, thus eliminating the reason for the development of this instability. A signification dilution of the active medium of a DF laser with helium up to the atmospheric pressure allowed us to achieve the limiting discharge initiation frequencies with the active medium replacement ratio $K \sim 1$.**

Keywords: *gas-dynamic perturbations, thermal plug, shock waves, overheat instability.*

1. Introduction

Despite their almost 50-year history, electric-discharge repetitively pulsed chemical HF(DF) lasers still attract the attention of researchers [1–14]. This is simply explained by the absence of really competitive sources with comparable peak and average output powers in the practically important wavelength range $\lambda = 2.6$–4.2 μm.

The development of efficient repetitively pulsed HF(DF) lasers with high average powers runs into the problem common for all electric-discharge repetitively pulsed lasers, namely, the discharge initiation repetition rate f_{max} is K-fold lower than the theoretically possible rate determined by the rate of gas replacement in the discharge gap $f_0 = v/b_0$ (v is the average active medium flow rate in the discharge gap and b_0 is the initiation region width) [14]. In other words, to maintain stable repetitively pulsed laser operation at a required initiation pulse repetition rate, it is necessary to pump the active mixture through the discharge gap with a rate $v = Kfb_0$. (Since the product fb_0 determines the flow rate needed for a single replacement of the active medium in the discharge gap for the time interval between initiation pluses, the coefficient K was named the active medium replacement ratio.) This situation is caused by the perturbations of the active mixture density, or the gas-dynamic perturbations due to repetitively pulsed initiation [15–25].

Since the gas-dynamic perturbations propagate upstream and must be removed from the discharge gap to the beginning of the next pulse, the typical value of K turns out to exceed two. In particular, The authors of [6] report a DF laser with the pulse repetition rate $f \leqslant 1200$ Hz at $K \approx 2.3$. Work [3] presents the results of investigation of a HF laser with the initiation rate $f \leqslant 2400$ Hz at $K \approx 5$. The authors of [14] noted that the coefficient K also increases with increasing limiting pulse repetition rate and changes from $K \approx 3$ for $f \approx 100$ Hz to $K \approx 5$ for $f = 1000$ Hz. In [26], as the maximum pulse repetition rate of a KrF laser increased from ~1000 to 5000 Hz, the coefficient K increased from 2.2 to 3.6 due to an increase in the gas mixture flow rate.

Among the main reasons for the appearance of perturbations of the working mixture density in electric-discharge lasers, one distinguishes the following: the ever-present inhomogeneity of the gas flow rate field in the discharge gap; the gas density fluctuations, which take place even in isothermal flows and are related to the flow rate pulsations [15]; the existence of boundary layers on electrodes [16–18]; the development of a temperature boundary layer due to increased energy deposition in the near-electrode regions [15]; the isentropic expansion of the thermal plug and the heat conduction; the increase in the size of the heated gas plug along the flow [14, 16–20]; gas heating by shock waves formed due to the pulsed energy deposition into the discharge [16, 19]; and the resonance acoustic waves [6, 15, 17, 21–25]. It is obvious that, due to different gas-dynamic characteristics of media, specific energy depositions, discharge formation systems, etc., the role of each of the factors is different in CO_2 and HF(DF) lasers, excimer lasers, and gas lasers of other types.

For the repetitively pulsed HF(DF) laser, on the one hand, the authors of [6] claim that the factor responsible for a decrease in the average pulse energy with increasing initiation frequency and for a much lower maximum initiation frequency than the limiting value is the existence of acoustic perturbations. There, it was emphasised that an efficient method for their suppression is to increase the sound velocity in the working mixture by diluting it with a light gas (helium). On the other hand, in [14], the main role is assigned to the isentropic expansion of the thermal plug and to the existence of a temperature boundary layer at the electrodes. In the same

P.A. Evdokimov, D.V. Sokolov Russian Federal Nuclear Center 'All-Russian Research Institute of Experimental Physics', prosp. Mira 37, 607190 Sarov, Nizhnii Novgorod region, Russia;
e-mail: oefimova@otd13.vniief.ru

Received 4 March 2015; revision received 10 April 2015
Kvantovaya Elektronika **45** (11) 1003–1009 (2015)
Translated by M.N. Basieva

work, it was noted that the influence of such factors as the gas heating by shock waves and the excitation of acoustic waves is usually considerably weaker. Publication [27] presents the experimental results on a HF(DF) laser in which the maximum initiation pulse repetition rate for the SF_6-D_2-He active medium at the atmospheric pressure was increased to 2000–2200 Hz compared to the rate 600–700 Hz for the SF_6-D_2 active medium. In this case, the active mixture replacement ratio is $K \approx 1.2$, which confirms the conclusions made in [6] on a positive effect of addition of He to the working medium of the HF(DF) laser in order to achieve the limiting initiation pulse repetition rate and to suppress gas-dynamic perturbations. In this connection, it is of undoubted interest to quantitatively estimate the perturbations of one or another nature in the active media of both compositions under identical initiation conditions, as well as to try to answer the question about the role played by He in the suppression of gas-dynamic perturbations in HF(DF) lasers.

The present work continues the investigations performed in [27]. All the energy and technical characteristics of the experiments presented in this paper completely correspond to those used in [27].

2. Experimental setup

The experimental part of the work is performed on an electric discharge closed-cycle HF(DF) laser with a ring gas-dynamic circuit, which is described in detail in [27]. For pulsed initiation, we used a bulk discharge formation system with a discharge gap cross section of 10 × 10 mm and with the active mixture preionisation by the UV radiation of coupled capacitive discharges. The investigations were performed for two active mixture compositions, namely, the first composition was free of He (total gas pressure $p_{mix} = 0.18$ atm), and the second composition was diluted with He to the atmospheric pressure. The ratio of the active components was identical for both compositions ($SF_6 : D_2 = 6 : 1$), while the ratio of partial pressures for the medium with the atmospheric pressure was $(SD_2 + D_2) : He = 0.09 : 0.91$ atm. The specific energy deposition into the discharge ω_{dis} was constant and equal to ~40 J L^{-1}. Taking into account the chemical reaction, the total specific energy release in the discharge gap is $\omega_{dis} \approx 42.5$ J L^{-1}. For the first and second compositions, the active gas flow rates in the discharge gap are approximately 27 and 25 m s^{-1}, while the limiting initiation rates are about 700 and 2200 Hz, respectively [27].

The perturbations of the active medium density in the discharge gap were experimentally recorded by laser interferometry. All the experiments were conducted using an interferometer assembled according to the classical scheme of the two-beam Michelson interferometer. The interference pattern resulted from summing of the reference and probe beams was build up directly on the matrix of a pco.dimax high-speed CCD camera. Depending on the experimental conditions, we used two recording regimes: with a frame repetition rate of 5 kHz and an exposure time of 40 μs for a pulsed discharge in the motionless mixture of the DH laser and with a frame repetition rate of 25 kHz and an exposure time of about 8 μs for a pulsed discharge in flowing gas.

The laser beam in [27] was confined by an aperture 10 × 10 mm, because of which all the characteristics calculated from the interference patterns were accurate up to a constant. The disposition of electrodes on the interference patterns was as follows: the cathode was at the top and the anode was at the bottom.

3. Experimental results

3.1. Pulsed discharge in a gas at rest

The study of the interference patters observed under the condition of a pulsed discharge in the motionless mixture allows one both to determine the character and localisation of gas-dynamic perturbations themselves and to find their source. Figures 1 and 2 present the interference patterns of gas-dynamic perturbations at a pulsed discharge in the active medium of both compositions.

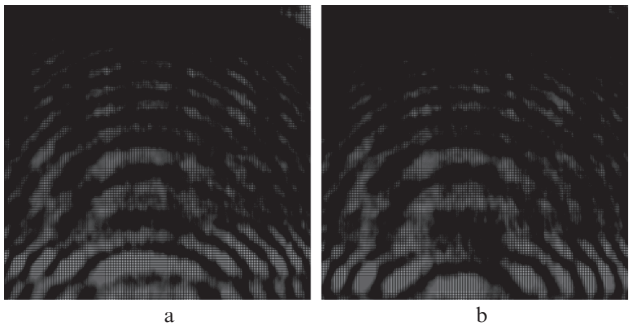

Figure 1. Interference patterns of the discharge gap at the instants $t =$ (a) 1.2 and (b) 1.8 ms after the initiation pulse for the SF_6-D_2 working mixture.

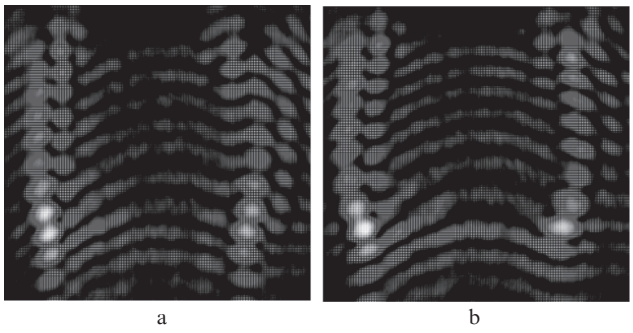

Figure 2. Interference patterns of the discharge gap at the instants $t =$ (a) 0.2 and (b) 1.0 ms after the initiation pulse for the SF_6-D_2-He working mixture.

Analysis of the images allows us to conclude that two groups of perturbations exist in both cases. The first, general group includes large-scale perturbations over the entire discharge gap cross section, which are observed as a considerable shift of the interference bands and are related to the expansion of the heated gas plug. The second group contains the perturbations which result from the energy deposition inhomogeneities over the discharge gap cross section and are different for these compositions. The perturbations typical for the SF_6-D_2 working mixture are related to a higher energy release near the electrodes and to the formation of electrode shock waves. In the case of a pulsed discharge in the SF_6-D_2-He working medium, there are no perturbations caused by the inhomogeneous distribution of energy deposi-

tion along the discharge gap height, but there exist perturbations testifying to inhomogeneity of the energy deposition near the discharge edges and are caused by field sharpening at the electrode edges.

Figures 3 and 4 show the dependences of the gas density in a probe window along the discharge gap height in the plane passing through the centre of electrodes, which were determined by processing the interferograms at different instants after the discharge pulse in the SF_6-D_2 and SF_6-D_2-He mixtures. One can see that, in the process of thermal expansion in the SF_6-D_2 mixture, the position of the maximum rarefaction shifts to the cathode, which may point to a higher energy release near the electrodes and to the existence of hot near-electrode layers. In particular, according to estimates of [18], a pulsed discharge in, for example, N_2 may cause an increase in the gas temperature near the cathode up to 1000 K, while a discharge in CO_2 may lead to even higher temperatures.

The change in the gas density in the discharge gap is related to the gas expansion caused by a pressure (temperature) jump upon the pulsed initiation and to the subsequent density recovery due to convective heat exchange. Since the energy release in the form of heat in a pulsed discharge occurs faster (almost immediately, for about 10^{-7} s) than the gas-dynamic perturbations propagate, the gas temperature jump in the initiation volume takes place at a constant volume, while the expansion of the heated gas plug is described by adiabatic equations.

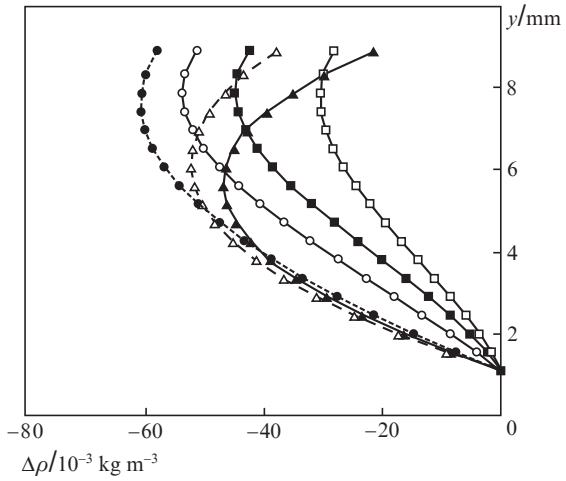

Figure 3. Distribution of the gas density variation $\Delta\rho$ along the discharge gap height ($x = 0$) at different instants t after a pulsed discharge in the SF_6-D_2 mixture: t = (▲) 5, (△) 20, (●) 50, (○) 70, (■) 100 and (□) 150 ms.

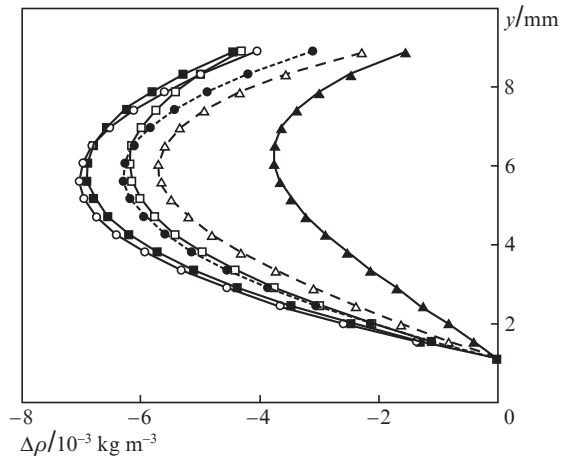

Figure 4. Distribution of the gas density variation along the discharge gap height ($x = 0$) at different instants t after a pulsed discharge in the SF_6-D_2-He mixture: t = (▲) 1, (△) 3, (●) 5, (○) 10, (■) 50 and (□) 100 ms.

The fact that the transverse size of the thermal plug b_0 is much smaller than its length allows one to consider the thermal expansion only in the transverse direction. The thermal plug size b_0 corresponds to the width of the energy deposition region and is smaller than the width of the electrodes. Assuming that, in the process of expansion, the thermal plug does not leave the boundaries of the electrodes, we ignore the change in the plug volume due to a change in its cross section caused by the electrode profile effect and, hence, write $V/V_0 = b/b_0$ (where V_0 and V are the thermal plug volumes before and after expansion and b is the transverse size of the thermal plug after expansion). From the condition of adiabaticity of the process, it follows that

$$p_p b_0^{\gamma} = p_0 b^{\gamma}, \tag{1}$$

where p_0 and p_p are the initial pressures in the flow and in the thermal plug and γ is the adiabatic index. Using the ideal gas state equation, we obtain

$$\frac{b}{b_0} = \frac{T_h}{T_0} = \left(1 + \frac{\Delta T}{T_0}\right)^{1/\gamma}, \tag{2}$$

where T_0 and T_h are the initial gas temperature in the initiation volume and the plug temperature after expansion, and ΔT is the gas temperature jump in the initiation volume.

Since the specific heat capacity of a material in the general case depends on temperature, the temperature jump of the heated gas can be determined by solving the integrodifferential equation

$$\int_{T_0}^{T_p} c_V(T)\,\mathrm{d}T = \frac{W}{m}, \tag{3}$$

where T_p is the final gas temperature in the initiation volume, $c_V(T)$ is the specific isochoric heat capacity of the medium, and m and W are the gas mass and the total energy release in the initiation volume.

We determined the temperature dependences of the specific isochoric heat capacity of the SF_6-D_2 and SF_6-D_2-He working mixtures based on the data of specific molecular heat capacities for the mixture components He [28], D2 [29], and SF6 [30] at a constant pressure $c_p(T)$. At the total (with allowance for the discharge and the chemical reaction) specific energy release $\omega_{dis} \approx 42.5$ J L^{-1}, the gas temperature in the initiation volume increases approximately by 68 and 51.7 K for the SF_6-D_2 and SF_6-D_2-He working media, respectively.

Table 1 lists the following thermodynamic characteristics of the mixtures: γ_0 and a_0 for the initial temperature $T_0 = 300$ K, γ_p and a_p for the thermal plug temperature T_p, and γ_h and a_h for the thermal plug temperature T_h after adiabatic expansion. Here, a_0, a_p and a_h are the sound velocities corresponding to the above-mentioned temperatures.

The fraction of energy released in the discharge and spent on increasing the internal gas energy in the thermal plug volume is

Table 1. Thermodynamic characteristics of the mixtures.

Working mixture	T_0/K	γ_0	a_0/m s^{-1}	T_p/K	γ_p	a_p/m s^{-1}	b/b_0	T_h/K	γ_h	a_h/m s^{-1}
SF_6–D_2	300	1.1007	149.65	368.0	1.0914	165.04	1.21	361.6	1.0921	163.65
SF_6–D_2–He	300	1.4114	454.51	351.7	1.3974	489.67	1.12	336.2	1.4013	479.43

$$\delta Q = \frac{T_h - T_0}{T_p - T_0}. \quad (4)$$

From this, taking into account the thermal plug temperatures before and after expansion, we have $\delta Q \approx 0.9$ for the SF_6–D_2 active mixture and 0.7 for the working mixture at the atmospheric pressure. In other words, while about of 30% of energy released in the discharge gap at the atmospheric pressure is removed by shock waves, the energy released in the SF_6–D_2 mixture is almost completely spent on increasing the internal gas energy, and the fraction of energy taken away by shock waves is ~10%.

The temperature (and, correspondingly, pressure) jump at the boundary between cold and heated gas leads to the formation of a region of a break in the gas-dynamic characteristics and to the appearance of a shock wave. The equations describing the relation of the shock wave Mach number with the cold and heated gas parameters based on the theories of shock waves and self-similar motion of a polytropic gas [31, 32] have the form [32, 33]

$$\left(1 - \frac{\gamma_p - 1}{\gamma_p + 1}\frac{a_0}{a_p}\frac{M^2 - 1}{M}\right)^{2\gamma_p/(\gamma_p - 1)} = \frac{T_0}{T_p}\frac{1}{\gamma_0 + 1}[\gamma_0(2M^2 - 1) + 1], \quad (5)$$

$$u = Ma_0\frac{2(M^2 - 1)}{M^2(\gamma_0 + 1)}, \quad M = \frac{D}{a_0}, \quad (6)$$

where D is the shock wave velocity and u is the velocity of motion of the contact surface between compression and rarefaction jumps.

Table 2 presents the thermodynamic characteristics of the mixtures in the compression (ρ_1, p_1,T_1) and rarefaction (ρ_2, $p_2 = p_1$, T_2) regions (ρ_1 and ρ_2 are the densities of the mixtures in the corresponding regions). One can see that the scale of gas-dynamic perturbations caused by a pulsed discharge is almost the same for both compositions of the working mixture of the DF laser. Therefore, they play identical roles in the restriction of the maximum initiation repetition rate. Thus, since they exert no restricting effect in DF lasers with the SF_6–D_2–He working medium, then they also must not limit the initiation repetition rate in DF lasers with the SF_6–D_2 mixture.

3.2. Pulsed discharge in the active mixture flow

Figure 5 presents the interference patterns observed in the axial plane of the discharge gap (probe window height is 1.1 mm) at different time moments with respect to the pulsed discharge instant in the flow of the active medium of the DF laser. It is seen that, despite the difference in the character of the motion of the hot region boundary, the time of the thermal plug removal from the discharge gap is approximately the same (~0.36 ms) for both active mixtures and is completely determined by the average flow rate.

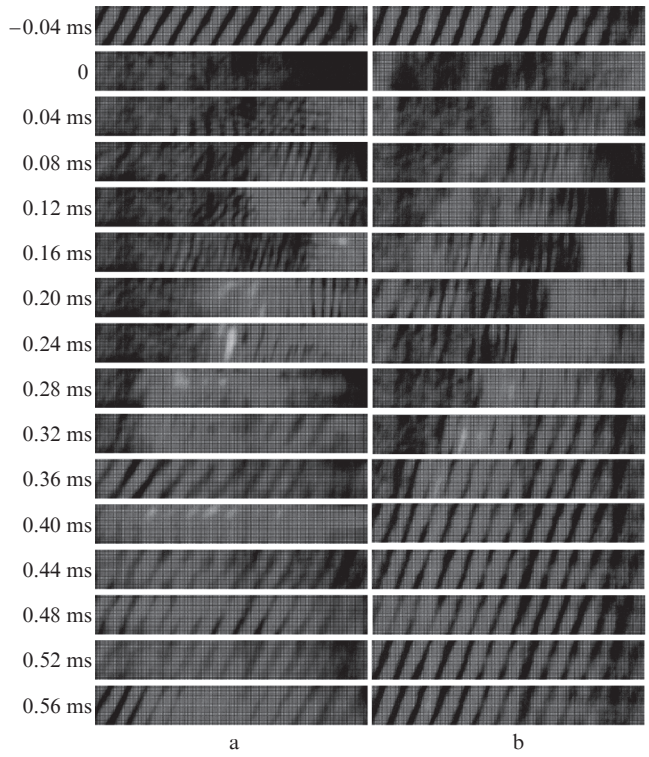

Figure 5. Interference patterns of the discharge gap in the axial plane recorded at different time moment t with respect to a pulsed discharge in the flow of the (a) SF_6–D_2 and (b) SF_6–D_2–He active mixtures of the DF laser.

In [29], the vibrational character of the gas flow (mixture SF_6 : D_2 = 9 : 1, total pressure p_{mix} = 0.1 atm, initiation repetition rate f = 17 Hz, gas flow rate v = 1.4 m s^{-1}) is explained by acoustic waves propagating along the flow, their reflection from the ends of the gas-dynamic channel, and the superposition of acoustic perturbations – compression and rarefaction waves. In our case, under the conditions of single initiation, a curved (ring) gas-dynamic channel, a ventilation unit from one side and a filter with a porous structure from the other side, this explanation seems low probable due to qualitative estimates in Section 3.1. A more probable reason is the difference in the intensities of the thermal expansion of the heated gas plug ($\gamma \approx 1.1$ for one medium and 1.4 for the other) and

Table 2. Parameters D, u and thermodynamic characteristics of media corresponding to compression (ρ_1,p_1,T_1) and rarefaction (ρ_2,$p_2 = p_1$,T_2) regions.

Working mixture	D/m s^{-1}	u/m s^{-1}	ρ_1/ρ_0	p_1/p_0	T_1/T_0	ρ_2/ρ_0	T_2/T_0
SF_6–D_2	157.52	14.61	1.1022	1.1131	1.0098	0.9148	1.2167
SF_6–D_2–He	470.84	26.62	1.0599	1.0856	1.0242	0.9465	1.1470

the gas-dynamic resistance of the thermal plug to the flow. As a characteristic of this resistance, one can consider the ratio of the deposited energy to the internal flow energy in the discharge region,

$$\omega' = W\left(\frac{p_0 V}{\gamma_0 - 1}\right)^{-1}. \quad (7)$$

Taking into account that a part of the deposited energy is removed by shock waves, this ratio is about 0.23 and 0.13 for the SF_6-D_2 and SF_6-D_2-He active mixtures, respectively.

From Fig. 5, one also sees that, after removal of the thermal plug from the discharge gap, beginning from the time moment 0.36 ms, the period of interference fringes in horizontal planes does not change any more, which testifies to the absence of gas mixture perturbations propagating along the flow. At the same time, the interference pattern of the SF_6-D_2 mixture at the time moment 0.4 ms demonstrates the propagation of density perturbations in the direction perpendicular to the flow (and parallel to the electrodes), which is related to a higher energy release near the electrodes and to the formation of electrode shock waves (see Fig. 1).

3.3. Gas heating by shock waves

As a result of pulsed initiation, part of the deposited energy is released in the form of heat and part is removed by shock waves. As follows from relation (4), the energy fraction W_w/W removed by shock waves is approximately equal to 0.1 and 0.31 for the SF_6-D_2 and SF_6-D_2-He mixtures, respectively. Thus, while up to 30% of the deposited energy in the SF_6-D_2 medium is removed by shock waves and about 69% is spent on heating, these values for the SF_6-D_2 medium are about 10% and 90%, respectively.

The authors of [15, 18] analyse gas heating by shock waves. As the upper estimate, they suggest the following expression for calculating the maximum possible gas temperature under the condition that all energy removed by shock waves is released in the gas:

$$\frac{T_{max}}{T_0} = 1 + \frac{1}{2}\frac{W_w}{W}\frac{b_0}{v\tau}\frac{\gamma - 1}{\gamma}\frac{\omega}{p_0}, \quad (8)$$

where τ is the pulse repetition period. Then, for limiting frequencies of 700 and 2000 Hz [27], we have $T_{max}/T_0 \approx 1.003$ for the SF_6-D_2 mixture and 1.013 for SF_6-D_2-He.

From this estimate, one can see that, for both active mixture compositions, the density gradients appearing at this heating are too small to play an important role in the distortion of the discharge homogeneity and in limiting the maximum initiation frequency.

3.4. Resonance acoustic waves

Studying the problem of the theoretical upper limit of the pulse repetition rate of repetitively pulsed lasers, which is determined by the time of the thermal plug removal from the discharge gap, one almost always considers the resonance acoustic wave as one of the main reasons for this limiting [21]. At the same time, it was noted [6] that an efficient method of suppressing acoustic waves is an increase in the sound velocity in the active medium by diluting it with helium.

Let us consider how strongly acoustic waves can affect the operation of repetitively pulsed DF lasers and what role is played in this process by the dilution of the active medium with helium. First, let us list some of the results obtained above:

(1) The time of the thermal plug removal from the discharge gap is approximately the same for both active mixture compositions and is determined by the average flow rate in the axial plane of the discharge gap.

(2) The upper estimates of the shock wave energy density for the SF_6-D_2 and SF_6-D_2-He mixtures are 2.4 and 6.7 mJ $\times$ cm^{-2}, respectively.

(3) The sound velocity in the SF_6-D_2-He working mixture (about 454.5 m s^{-1}) is higher than in the SF_6-D_2 mixture (about 149.7 m s^{-1}) approximately by a factor of three, and the ratio of the shock wave energy densities in these media is the same.

(4) The limiting initiation frequency for a DF laser with the SF_6-D_2-He working medium is 2200 Hz [27] and is approximately equal to the frequency limited by the time of the thermal plug removal. The limiting initiation frequency for a DF laser with the SF_6-D_2 active mixture is about 700 Hz and more than by 3.5 times lower than the frequency limited by the time of the thermal plug removal.

The formation of weak shock waves in working media of gas lasers as a result of pulsed initiation is an undeniable fact and cannot be in doubt. Having low amplitudes, these waves rapidly transform into acoustic waves. In particular, in the case of the DF laser in [8], the shock wave Mach numbers are 1.05 and 1.03 for the SF_6-D_2 and SF_6-D_2-He working mixtures, respectively. In the process of propagation in the gas channel, acoustic waves decay by two ways, namely, they are absorbed in matter and lose their energy upon reflections from the gas channel elements.

The absorption of a plane acoustic wave with the amplitude A_0 in matter is described by the equation

$$A_d = A_0 \exp(-\alpha d), \quad (9)$$

where A_d is the wave amplitude at the distance d,

$$\alpha = \frac{2\pi^2 v^2}{a^3 \rho}\left(\frac{4}{3}\eta + \frac{\gamma - 1}{c_p}\chi\right) \quad (10)$$

is the acoustic wave absorption coefficient, v is the sound frequency, a is the sound velocity, η is the dynamic viscosity coefficient, and χ is the thermal conductivity.

As is seen from (10), $\alpha \propto a^{-3}$, and the efficiency of acoustic wave absorption in matter decreases with increasing sound velocity. The dependence of coefficient α on other parameters is insignificant for the considered problem. Thus, the efficiency of absorption of acoustic waves in the SF_6-D_2 mixture is higher than in SF_6-D_2-He (in the case of equality of their frequencies), but, nevertheless, the limiting initiation frequency in SF_6-D_2 is lower. Therefore, the increase in the sound velocity due to dilution of the working medium with helium cannot be the factor allowing one to achieve the desired increase in the limiting initiation frequency. For example, in [24], it is directly shown that the efficiency of excitation of an acoustic wave and its decay rate at low flow Mach numbers ($M \ll 1$) do not depend on M, i.e., the role of the flow at $M \ll 1$ is reduced to the thermal plug removal and only slightly affects both the longitudinal and transverse acoustic vibrations.

Let us consider the energy losses due to the reflection from the gas channel elements. The acoustic wave reflection and

propagation coefficients depend on the ratio of wave resistances of the two media, and the wave resistances, in turn, are proportional to the acoustic resistances. The wave resistance of gases is much lower than that of solids, because of which a wave incident from gas on a solid barrier (whose thickness in the wave propagation direction is large) is almost completely reflected. If the barrier thickness is much smaller that the sound wavelength in the barrier, then the reflection coefficient is low and the propagation coefficient is high. The main materials of gas channel elements are alloys with a high concentration of aluminium. The sound velocity in aluminium is approximately 6420 m s^{-1}. The acoustic vibrations with frequencies of 14 and 43 kHz and a wavelength in the gas equal to the width of the electrodes have the wavelengths in aluminium of 0.45 and 0.15 m. Since the characteristic thicknesses of the laser units do not exceed 5 mm, the acoustic waves will identically efficiently propagate through metal barriers with only weak reflection.

Thus, the above considerations show that the effect of resonance acoustic waves in a DF laser at a specific energy deposition of about 40 J L^{-1} is identical for the working media of both compositions and does not explain the restriction of the maximum initiation frequency for the SF_6-D_2 mixture to a value considerably lower than the limiting frequency.

3.5. Development of a temperature boundary layer

A boundary layer formed when gas flows around a wall decreases the efficiency of replacement of a working mixture in the near-electrode region. The interferometric studies and the numerical simulation performed in [27] for a DF laser showed that the thickness of the boundary layer on the plane region of electrodes is approximately the same for both active compositions (~0.5 mm). The effect of these layers for the interelectrode gap with a width of 10 mm can be noticeable, especially in the case of higher energy depositions in the near-electrode region. For example, the authors of [18] reported that, as applied to their setup, the density inhomogeneities appearing in the boundary layers turn out to be an order of magnitude higher than the inhomogeneities related to acoustic waves.

As was noted above, the typical perturbations for a pulsed discharge in the SF_6-D_2 mixture are caused by an increased energy deposition near the electrodes and by the formation of electrode shock waves, which, under the conditions of inefficient energy exchange, can lead to the development of a temperature boundary layer, to overheating instability, and to limiting of the initiation pulse repetition rate. This is confirmed by the experiments on recording the DF laser radiation in the near-field zone. Figure 6 shows the near-field zone images (burns on carbon paper) obtained in a repetitively pulsed initiation regime for one second at a pulse repetition rate of 600 Hz, which is close to the maximum rate for DF lasers with the SF_6-D_2 active mixture. These experiments were performed with the anode at the top and the cathode at the bottom.

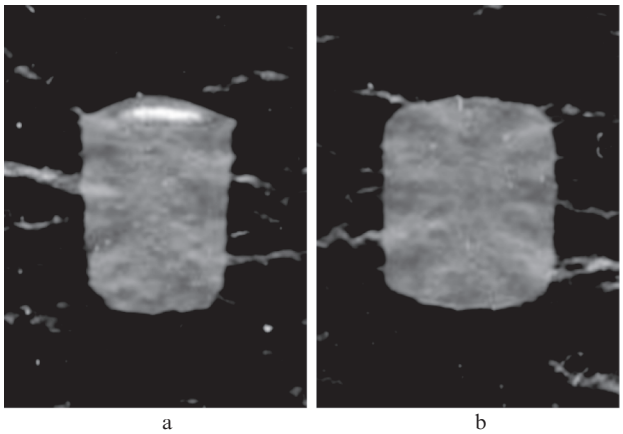

a b

Figure 6. Images of the near-field radiation zone for the DF laser (a) with the SF_6-D_2 active mixture at p_{mix} = 0.16 atm and (b) with the working mixture of the composition $(SF_6 + D_2)$: He = 0.09 : 0.91 atm.

In the case of a pulsed discharge in the SF_6-D_2 mixture (Fig. 6a), one can clearly see a pronounced near-anode region with increased energy deposition. The dilution of the working mixture with helium up to the atmospheric pressure (Fig. 6b) improves the discharge homogeneity, the region of increased energy deposition disappears, and the cross section geometry approaches the calculated parameters.

Thus, we proved the suggestion that the development of overheating instability, which is caused by a higher energy deposition near the electrodes and by the formation of electrode shock waves, is the factor that limits the maximum initiation pulse repetition rate of DF lasers with the SF_6-D_2 active mixture.

4. Conclusions

The quantitative analysis of perturbations in the active gas flow due to pulsed initiation showed that, at the specific energy deposition $\omega_{dis} \approx 40$ J L^{-1}, neither the isentropic expansion of the thermal plug nor the gas heating by shock waves can be the factors limiting the maximum initiation frequency of electric-discharge DF lasers with the SF_6-D_2 active mixture by a value considerably lower than the frequency determined by the gas flow rate and the width of the electrodes.

At the same time, our investigations revealed that a strong dilution of the working medium of the DF laser with helium up to the atmospheric pressure considerably changes the distribution of the specific energy deposition over the discharge gap cross section. Despite the fact that the pulsed discharge in the SF_6-D_2-He mixture at the atmospheric pressure is accompanied by an increase in the energy release at the discharge boundaries due to sharpening of the field at the edges of the electrodes, a more important, determining fact is that an improvement of the discharge homogeneity over the discharge gap height leads to the disappearance of the regions of higher energy deposition near the electrodes, with are typical for the discharge in the mixture without helium.

It is suggested that the increased energy deposition near the electrodes, which is typical for the discharge in the active mixture without helium, and the related formation of shock waves lead to the development of overheating instability, which limits the maximum initiation frequency of the DF laser with the SF_6-D_2 active mixture by a value considerably lower than the frequency determined by the time of the thermal plug removal from the discharge gap.

The role of He as an additive to the working medium of DF lasers consists in the change of the discharge structure and in the improvement of its homogeneity. Significant dilution of the active mixture of the DF laser with helium up to the atmospheric pressure allowed us to considerably improve

the discharge homogeneity along the discharge gap height, to exclude to reasons for the development of the near-anode overheating instability, and to achieve limiting initiation frequencies with the working gas replacement ratio $K \sim 1$.

References

1. Apollonov V.V., Kazantsev S.Yu., Oreshkin V.F., Firsov K.N. *Kvantovaya Elektron*., **25**, 123 (1998) [*Quantum Electron*., **28**, 116 (1998)].
2. Lacour B., Gadnol C., Priget P., Puech V. *Proc. SPIE Int. Soc. Opt. Eng*., **3574**, 334 (1998).
3. Lazhintsev B.V., Nor-Arevyan V.A., Selemir V.D. *Kvantovaya Elektron*., **30**, 7 (2000) [*Quantum Electron*., **30**, 7 (2000)].
4. Bulaev V.D., Kulikov V.V., Petin V.N., Yugov V.I. *Kvantovaya Elektron*., **31**, 218 (2001) [*Quantum Electron*., **31**, 218 (2001)].
5. Aksenov Yu.N., Borisov V.P., Burtsev V.V., Velikanov S.D., Voronov S.L., et al. *Kvantovaya Elektron*., **31**, 290 (2001) [*Quantum Electron*., **31**, 290 (2001)].
6. Butsykin I.L., Velikanov S.D., Evdokimov P.A., Zapol'skii A.F., Kovalev E.V., Kodola B.E., Pegoev I.N. *Kvantovaya Elektron*., **31**, 957 (2001) [*Quantum Electron*., **31**, 957 (2001)].
7. Apollonov V.V., Belevtsev A.A., Kazantsev S.Yu., Saifulin A.V., Firsov K.N. *Kvantovaya Elektron*., **32**, 95 (2002) [*Quantum Electron*., **32**, 95 (2002)].
8. Panchenko A.N., Orlovskii V.M., Tarasenko V.F. *Zh.Tekh. Fiz*., **73**, 136 (2003).
9. Bychkov Yu., Gortchakov S., Lacour B., Pasquires S., Puech V. *J. Phys. D. Appl. Phys*., **36**, 380 (2003).
10. Azarov M.A., Klimuk E.A., Kutumov K.A., Troshchinenko G.A., Lakur B. *Kvantovaya Elektron*., **34**, 1023 (2004) [*Quantum Electron*., **34**, 1023 (2004)].
11. Andramanov A.V., Kabaev S.A., Lazhintsev B.V., Nor-Arevyan V.A., Pisetskaya A.V., Selemir V.D. *Kvantovaya Elektron*., **36**, 235 (2006) [*Quantum Electron*., **36**, 235 (2006].
12. Bulaev V.D., Gusev V.S., Kazantsev S.Yu., Kononov I.G., Lysenko S.L., Morozov Yu.B., Poznyshev A.N., Firsov K.N. *Kvantovaya Elektron*., **40**, 615 (2010) [*Quantum Electron*., **40**, 615 (2010)].
13. Belevtsev A.A., Kazantsev S.Yu., Kononov I.G., Lebedev A.A., Podlesnykh S.V., Firsov K.N. *Kvantovaya Elektron*., **41**, 703 (2011) [*Quantum Electron*., **41**, 703 (2011)].
14. Velikanov S.D., Zapol'skii A.F., Frolov Yu.N. *Kvantovaya Elektron*., **24**, 11 (1997) [*Quantum Electron*., **27**, 9 (1997)].
15. Baranov V.Yu, Malyuta D.D., Mezhevov V.S., Napartovich A.N. *Kvantovaya Elektron*., **7**, 2589 (1980) [*Sov. J. Quantum Electron*., **10**, 1512 (1980)].
16. Baranov V.Yu, Breev V.V., Malyuta D.D., Niz'ev V.G. *Kvantovaya Elektron*., **4**, 1861 (1977) [*Sov. J. Quantum Electron*., **7**, 1059 (1977)].
17. Baranov V.Yu, Malyuta D.D., Mezhevov V.S. *Kvantovaya Elektron*., **5**, 2186 (1978) [*Sov. J. Quantum Electron*., **8**, 1234 (1980)].
18. Baranov V.Yu, Niz'ev V.G., Pigul'skii S.V. *Kvantovaya Elektron*., **6**, 177 (1979) [*Sov. J. Quantum Electron*., **9**, 97 (1979)].
19. Baranov V.Yu, Klepach G.M., Malyuta D.D., Mezhevov V.S., Niz'ev V.G., Chalkin S.F. *Teplofiz. Vys. Temp*., **15**, 972 (1977).
20. Borisov V.P., Burtsev V.V., Velikanov S.D., Vorontsov E.N., Elutin A.S., Zapol'skii A.F., Sinitsyn M.V., Frolov Yu.N., Shchurov V.V. *Kvantovaya Elektron*., **22**, 645 (1995) [*Quantum Electron*., **25**, 617 (1995)].
21. Vedenov A.A., Drobyazko S.V., Knizhnikov V.N., Turundaevskii V.B. *Teplofiz. Vys. Temp*., **13**, 425 (1975).
22. Baranov V.Yu., Lyubimov B.Ya., Niz'ev V.G., Pigul'skii S.V. *Kvantovaya Elektron*., **6**, 184 (1979) [*Sov. J. Quantum Electron*., **9**, 101 (1979)].
23. Baranov V.Yu., Borisov V.P., Vinokhodov A.Yu., Vysikailo F.I., Gubarev A.V., Kiryukhin Yu.B., Krayushkin I.E., Laptev S.A. *Kvantovaya Elektron*., **14**, 1206 (1987) [*Sov. J. Quantum Electron*., **17**, 766 (1987)].
24. Baranov V.Yu., Malyuta D.D., Mezhevov V.S., Napartovich A.N. *Fiz. Plazmy*, **6**, 785 (1980).
25. Baranov V.Yu., Borisov V.M., Vinokhodov A.Yu., Vysikailo F.I., Kiryukhin Yu.B. *Kvantovaya Elektron*., **10**, 540 (1983) [*Sov. J. Quantum Electron*., **13**, 318 (1983)].
26. Borisov V.M., Vinokhodov A.Yu., Vodchits V.A., El'tsov A.V., Ivanov A.S. *Kvantovaya Elektron*., **30**, 783 (2000) [*Quantum Electron*., **30**, 783 (2000)].
27. Velikanov S.D., Evdokimov P.A., Zapol'sky A.F., Kodola B.E., Sokolov D.V., Cernopyatov V.Y., Yakovlev E.D. *Proc. SPIE Int. Soc. Opt. Eng*., **7131**, 71310V (2008).
28. Kikoin I.K. (Ed.) *Tablitsy fizicheskikh velichin (spravochnik)* (Tables of Physical Quantities: A Handbook) (Moscow: Atomizdat, 1976).
29. Grigoriev I.S., Meilikhov E.Z. (Eds) *Handbook of Physical Quantities* (Boca Raton, NY, London: CRC Press, 1996; Moscow: Energoatomizdat, 1991).
30. Bortnik I.M. *Fizicheskie svoistva i elektricheskaya prochnost' elegaza* (Physical Properties and Electric Strength of Sulphur Hexafluoride) (Moscow: Energoatomizdat, 1998).
31. Zeldovich Ya.B., Raizer Yu.P. *Fizika udarnykh voln i vysokotemperaturnykh gidrodinamicheskikh yavlenii* (Physics of Shock Waves and High-Temperature Hydrodynamic Phenomena) (Moscow: Fizmatgiz, 2008).
32. Karnyushin V.N., Soloukhin R.I. *Makroscopicheskie i moleculyarnye protsessy v gasovykh sredakh* (Macroscopic and Molecular Processes in Gas Media) (Moscow: Atomizdat, 1981).
33. Belevtsev A.A., Kazantsev S.Yu., Kononov I.G., Firsov K.N. *Kvantovaya Elektron*., **36**, 646 (2006) [*Quantum Electron*., **36**, 646 (2006)].